Directional Modulation using Phased Arrays – Proof of Concept

Ben Goode

Cambridge Consultants

ben.goode@cambridgeconsultants.com

Abstract

Directional Modulation (DM) is a promising secure physical layer modulation technique able to maintain a low bit error rate (BER) transmission in only an intended target direction, whilst scrambling data in other directions. This is achieved by "on-the-fly" symbol-based modulation of a common carrier using the individual phase shifters on a phased array antenna. Furthermore, if data transmitted in this way is encrypted then the channel has two layers of security, having obvious application to defence and other secure communication markets.

Here, we present a proof-of-concept experiment to validate the theoretical background and then go on to explore how DM may be implemented practically under realistic constraints.

Introduction

Phased array antennas provide a method on-air RF signal combination that allows designers to manipulate the far-field radiation pattern of the antenna. Traditionally, this has been utilised to maximise radiation power in one direction whilst minimising it in all other directions, with the ability to steer the point of maximum power.

DM aims instead to steer the spatial point at which information can be coherently demodulated, whilst minimising the ability of users in all other directions to understand the transmission. Figure 1 shows an example of an ideal DM system transmitting QPSK data, where the intended receiver, Bob, sees an undistorted signal constellation on the IQ plane, whilst an eavesdropper, Eve, sees a scrambled constellation, making demodulation incredibly difficult.

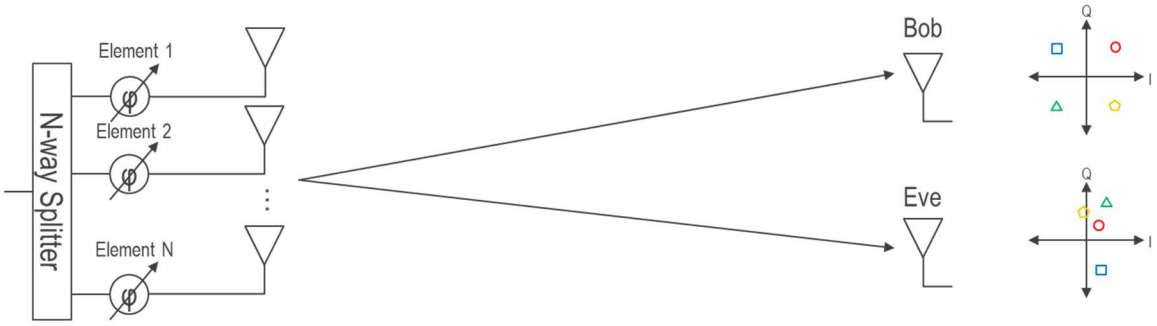

Figure 1 - Example of an ideal Directional Modulation transmission system.

Theoretical Basis

Phased Array Basics

To build understanding of how DM is achieved, it is useful to revisit a derivation of phased array behaviour from first principles. Consider a simple two element array as in Figure 2, where a common signal is split between two antenna chains, spaced apart by some distance, **d**, with uniform amplitude and some phase difference, $\Delta\Phi$, applied between them which steers the wavefront to some angle, θ. The value of $\Delta\Phi$ required to steer the wavefront to θ needs to be found.

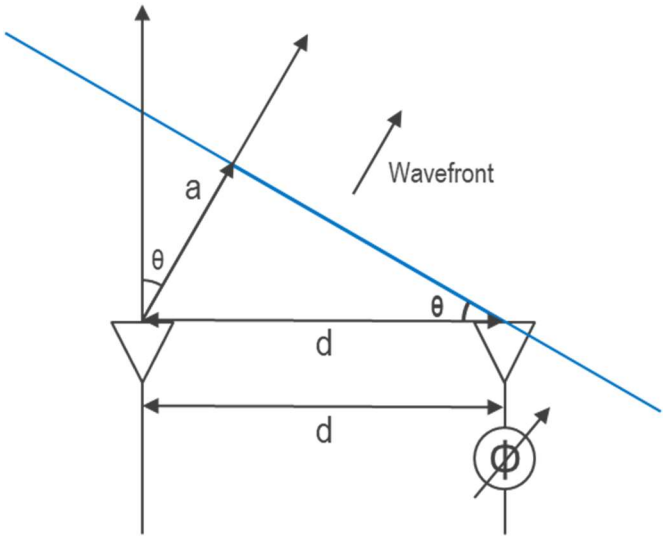

Figure 2 - Simple two element linear array.

The radiation from the first element has propagated a distance of **a** when the radiation from the second element begins to propagate, with a time delay of **Δt**. Since the waves travel at the speed of light, the distance **a** can be found as in (1).

$$a = c\Delta t \tag{1}$$

Now consider the right-angled triangle formed by **a**, **d** and the wavefront. Using simple trigonometry and rearranging, a second expression for **a** is shown in (2).

$$\sin\theta = \frac{a}{d} \therefore a = d\sin\theta \tag{2}$$

Returning to Figure 2, a phase shift can be related to a time delay using (3), and therefore using some substitution, (4) shows a relationship between ΔΦ and θ.

$$\Delta\Phi = 2\pi f\Delta t = \frac{2\pi c\Delta t}{\lambda} \tag{3}$$

$$\Delta\Phi = \frac{2\pi d\sin\theta}{\lambda} \tag{4}$$

A receiver in the far-field experiences the composite sum of the radiation from individual elements. If a phased array, with element spacing of λ/2, is steered such that the energy is maximum at boresight, no phase difference will be applied between the elements since the radiation from both elements needs to propagate at the same time.

A receiver that is 90° from boresight in this arrangement will receive the energy from the first element before that of the second element. Since the radiation from the second element has an additional distance of λ/2 to propagate, the two fields will always be in anti-phase and destructively interfere, meaning no energy will be seen by the receiver.

Therefore, the radiation seen at observation angle θ is a product of both the difference in phase due to the physical spacing between elements, ΔΦ, and the difference in phase applied to each element

to steer the wavefront to θ_0, $\Delta\phi$. Since the radiation pattern for an N element array is a composite sum, it can be modelled as array factor (i.e., discounting the radiation patterns of the individual elements for simplicity) in (5), where the phase shifts are represented as complex exponentials. Substituting in (4) yields (6), which shows that when observation angle is the same as steering angle, the exponential term cancels leaving a sum of 1's. Since each element in this array has a normalised magnitude of 1, this means the maximum power occurs at the steering angle, which is intuitively true.

$$AF(\theta) = \sum_{n=0}^{N-1} e^{-j\Delta\Phi} e^{j\Delta\varphi} \tag{5}$$

$$AF(\theta) = \sum_{n=0}^{N-1} e^{\frac{-j2\pi nd \sin\theta}{\lambda}} e^{\frac{2\pi nd \sin\theta_0}{\lambda}} = AF(\theta) = \sum_{n=0}^{N-1} e^{\frac{-j2\pi nd\,(\sin\theta - \sin\theta_0)}{\lambda}} \tag{6}$$

Therefore, for any observation angle, the far-field radiation pattern can be represented by a sum of N complex exponentials. Figure 3 shows the locus plot of (6) on the complex plane, with θ swept through ±90°. Figure 4 shows the magnitude of the same sweep against observation angle, which the most common way to represent the radiation pattern.

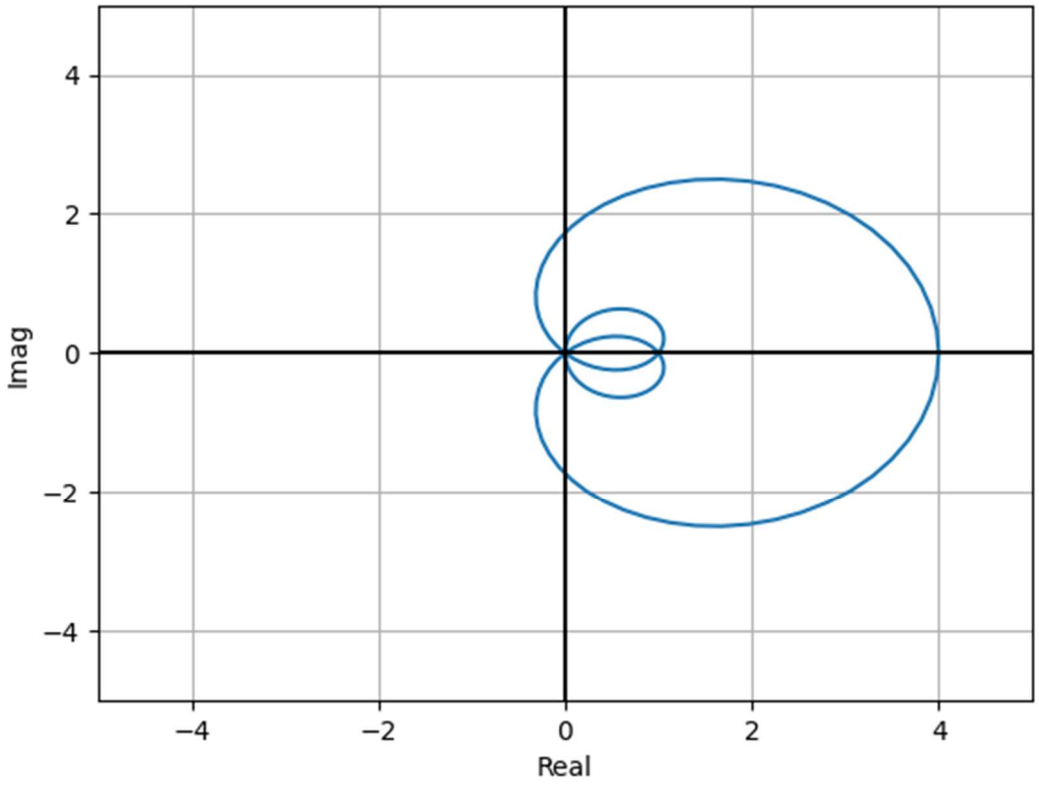

Figure 3 - Array factor of a four element linear array on the complex plane.

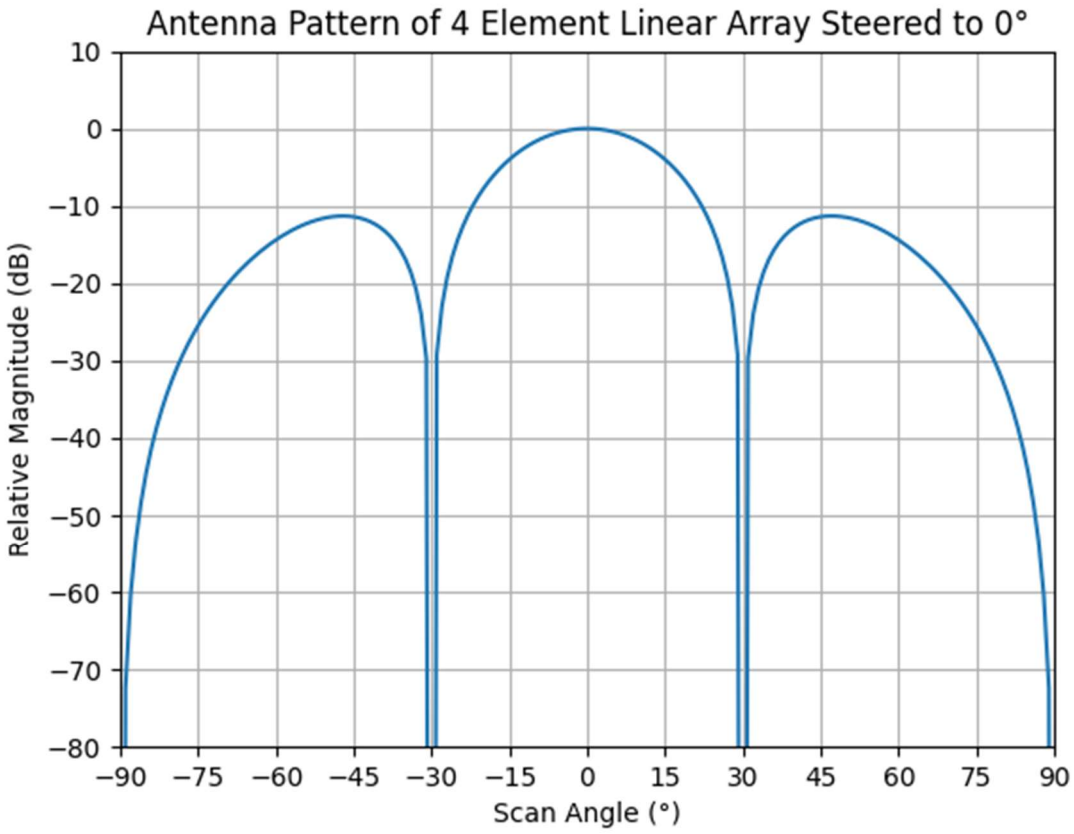

Figure 4 - Array factor of a four element linear array as magnitude in dB.

Directional Modulation Theory

Extracting the Δϕ term from (5) as the applied element phase shifts, this can be generalised as an element weighting function, **w(n)**, as in (7). As already shown, from the observation angle θ, the applied phase shifts are cancelled by the contribution from the physical spacing between elements and the resultant vector is 1 for all n. Therefore, with an additional element-wise phase shift applied as in (8), the relative far field phase can be controlled.

$$w(n) = e^{j\alpha} e^{\frac{j2\pi n d \sin\theta}{\lambda}} \tag{7}$$

Take for example a scenario where the relative phase of the far-field wavefront is steered to 45°. On the complex plane, this means the vectors need to sum to some multiple of 1+1j. To achieve this, the α values of the elements are selected to plot a path to the resultant complex point. In Figure 5, a 4-element linear array is used with a target complex phase point of 2+2j, by selecting two element α values of 0 and two element α of π (see (7)).

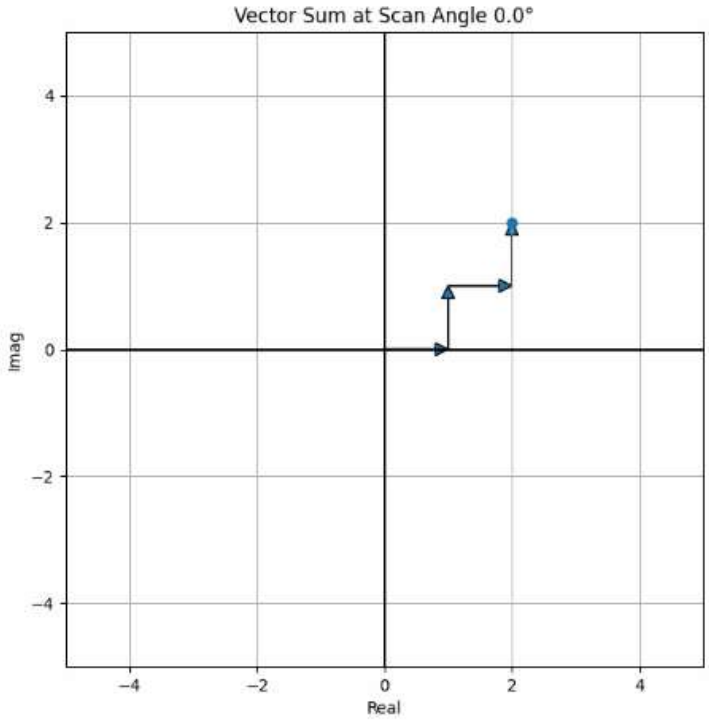

Figure 5 - Example of vector representation of element weightings to control far-field phase.

In Figure 6 and Figure 7, these weightings are shown in different orders, which yields the differing loci shown in Figure 8. Observing these loci at a set observation angle of 30° as shown in Figure 9, it's clear that while the phase is controlled for a receiver in the intended direction, it is randomised for receivers in other locations.

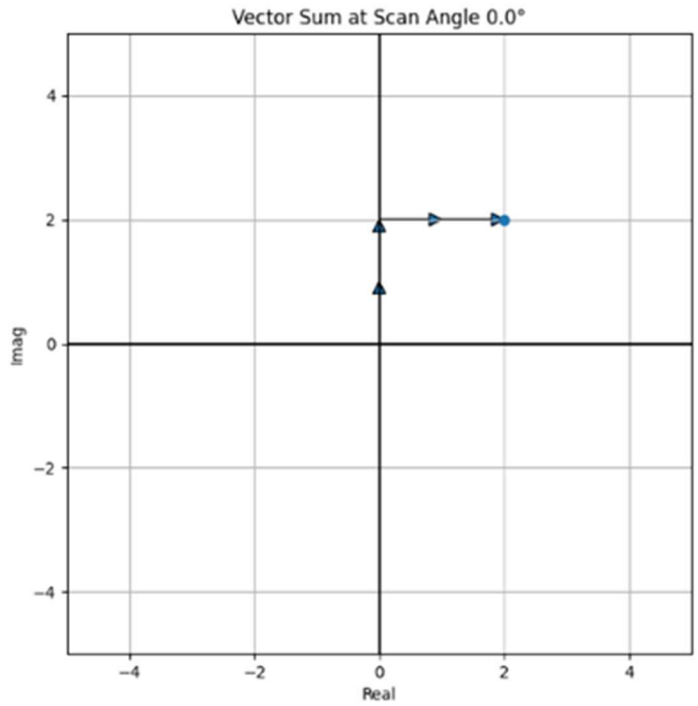

Figure 6 - Rearranged element weightings, first reconfiguration.

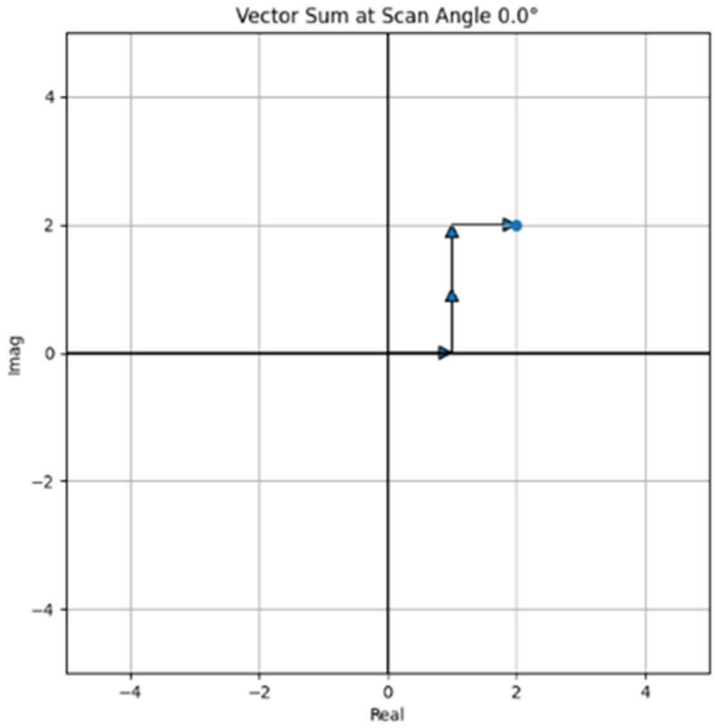

Figure 7 - Rearranged element weightings, second reconfiguration.

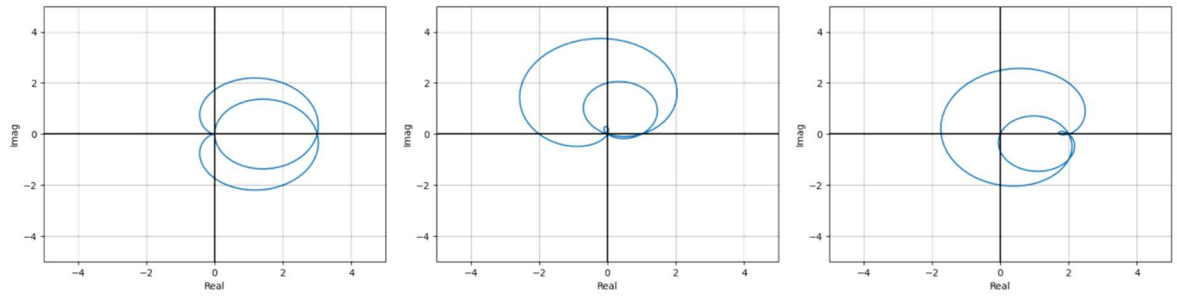

Figure 8 - Differing loci of rearranged element weightings as array factor.

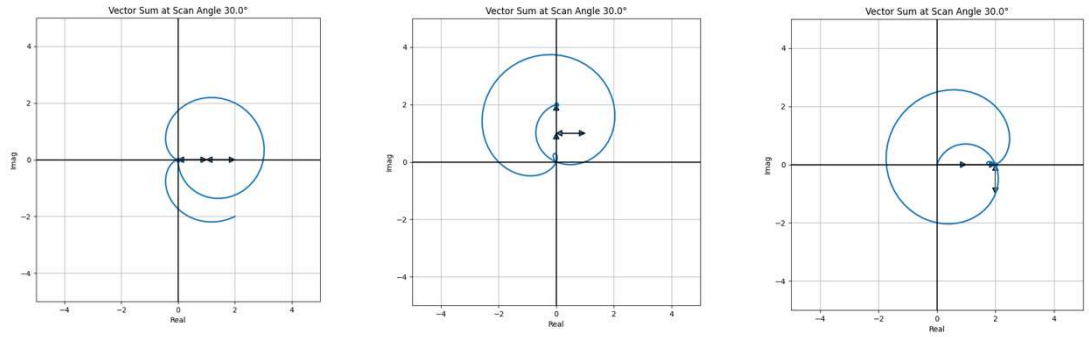

Figure 9 - Snapshot of array factor loci at observation angle of 30°.

Using this simple example, it is clear how the basis for the desired behaviour shown in Figure 1 is formed. A real array with digital phase shifters can therefore modulate a CW carrier and achieve a M-PSK modulation scheme by means of on-air signal combination.

Arrays with greater numbers of elements and finer phase shifter steps allow more precise control of the phase in the intended direction whilst offering greater randomisation, analogous to how arrays with more elements offer greater power and narrower beamwidth in traditional phased arrays.

Proof of Concept Experiment

Test Setup

The test configuration used is shown in Figure 10 and Figure 11. A 2.4GHz 4-channel phase shifter PCB module was designed, distributing a common source between 4 RF paths, each with a MACOM 6-bit phase shifter, allowing independent phase control down to 5.625° on each path. The phase shifters were controlled using a DIMAX SUB-20 board. This PCB was used to feed a 4-element linear array of monopole antennas, built using a large sheet of copper-lined FR4 and single-core wires tuned on a VNA by trimming the length. This assembly was placed on a turntable within an anechoic chamber to sweep observation angle.

The phase shifter PCB was fed by a signal generator, transmitting CW at 2.4GHz. The far field radiation from the array was measured using a horn antenna placed 4m from the array. The signal from the signal generator was coupled using a directional coupler to one port of a VNA, with the other port connected to the horn antenna.

The VNA was then used to compare the relative phase between the transmitted and received signal. To achieve this, the sweep mode was set to CW to only monitor the energy at 2.4GHz, and the measurement format was set to polar mode, which allowed for monitoring of the phase as if it were an IQ constellation point on the complex plane. To find the phase difference between the transmitted and received signal, a custom wave ratio was used, rather than a typical S-parameter measurement. Since only waves propagating into the VNA ports were of interest, the measurement was made on 'b' waves only, displaying the b_2/b_1 ratio. To normalise the phase difference, a trombone line stretcher was placed in the signal path from the signal generator and adjusted such that with all phase shifters set to 0°, the measurement on the VNA had 0° phase.

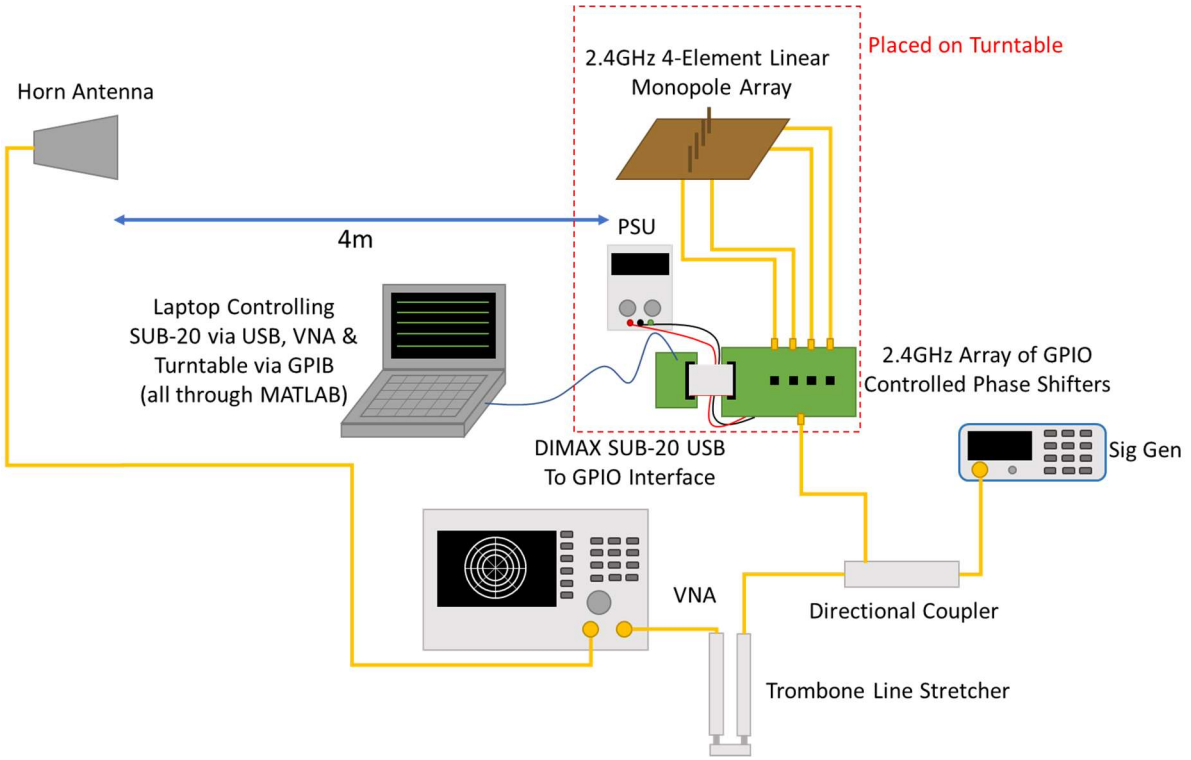

Figure 10 - Equipment setup for experiment.

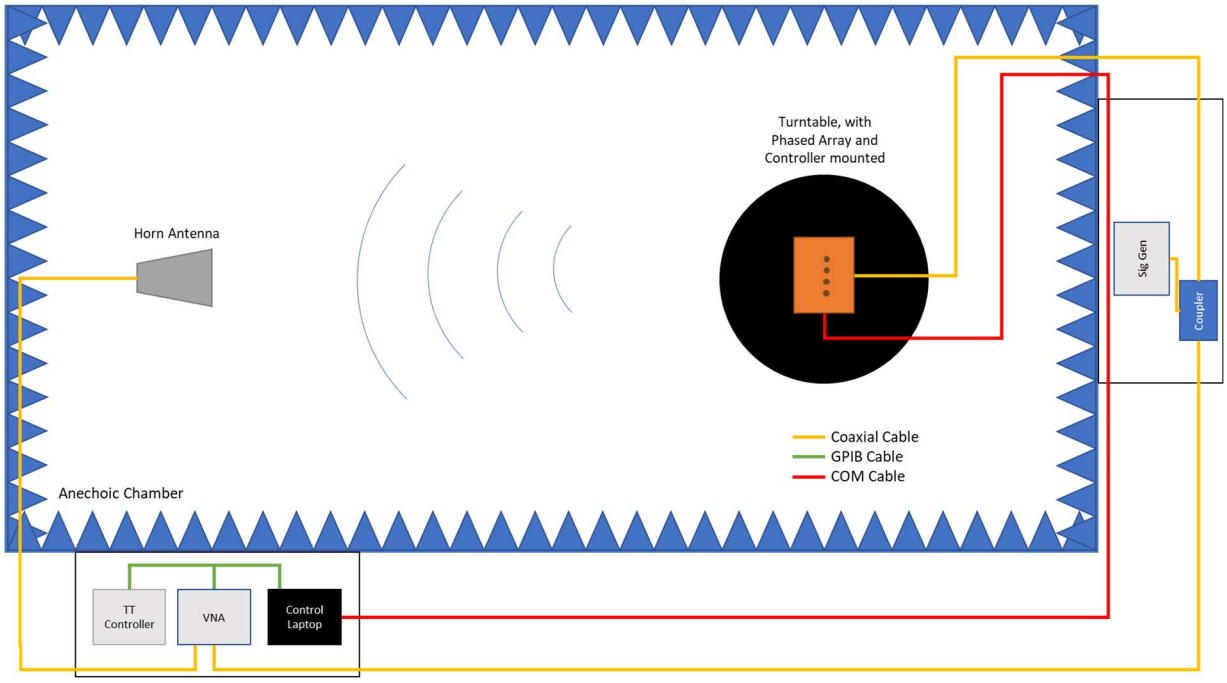

Figure 11 - Anechoic chamber test setup and layout.

Method

To emulate QPSK symbols, 8 combinations of element weightings were selected based on theory to give 2 different combinations of weightings per QPSK symbol. The first step in the experiment was to calibrate those weightings to account for slight differences in the electrical length of each channel due to factors such as cable variation between the board and the elements.

With the calibrated weightings, the turntable was swept through ±90° in 5° steps to vary the observation angle of the receiving antenna. At each observation angle, each of the 8 calibrated sets of element weightings was applied and the complex value of the wave ratio was recorded, allowing an overall array factor to be recorded for each weighting set.

This process was repeated using traditional phased array weightings, where all the phase shifters had the same phase, so the array was directed to boresight. For each QPSK symbol, the relative phase was emulated by applying that phase to all phase shifters, e.g. setting all phase shifters to 45° in order to steer the relative far-field phase to 45° like a QPSK symbol would appear, however since there is no difference in phase between elements, the beam is still steering in the correct direction.

Results

Figure 12 shows the comparison between the simulated and measured radiation patterns for each of the 8 DM symbols, shown as magnitude in dB. These show a good correlation considering the unrefined nature of the antenna array. This provides a good validation of the theoretical basis.

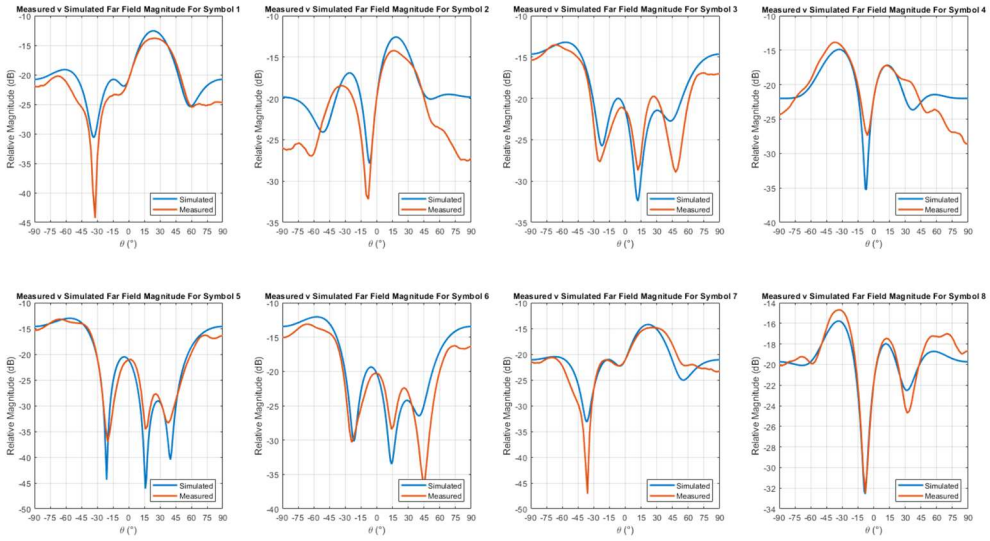

Figure 12 - Simulated and measured array patterns for eight DM weighting combinations.

The validation becomes even stronger when looking at Figure 13, which displays the received signals as constellation points in the intended direction, compared with Figure 14 and Figure 15, which show the same plots in unwanted directions. It is clear that a receiver along the intended direction would easily be able to demodulate this QPSK signal, whilst eavesdroppers off boresight would see a scrambled constellation where symbols have no relation to one another, making demodulation impossible.

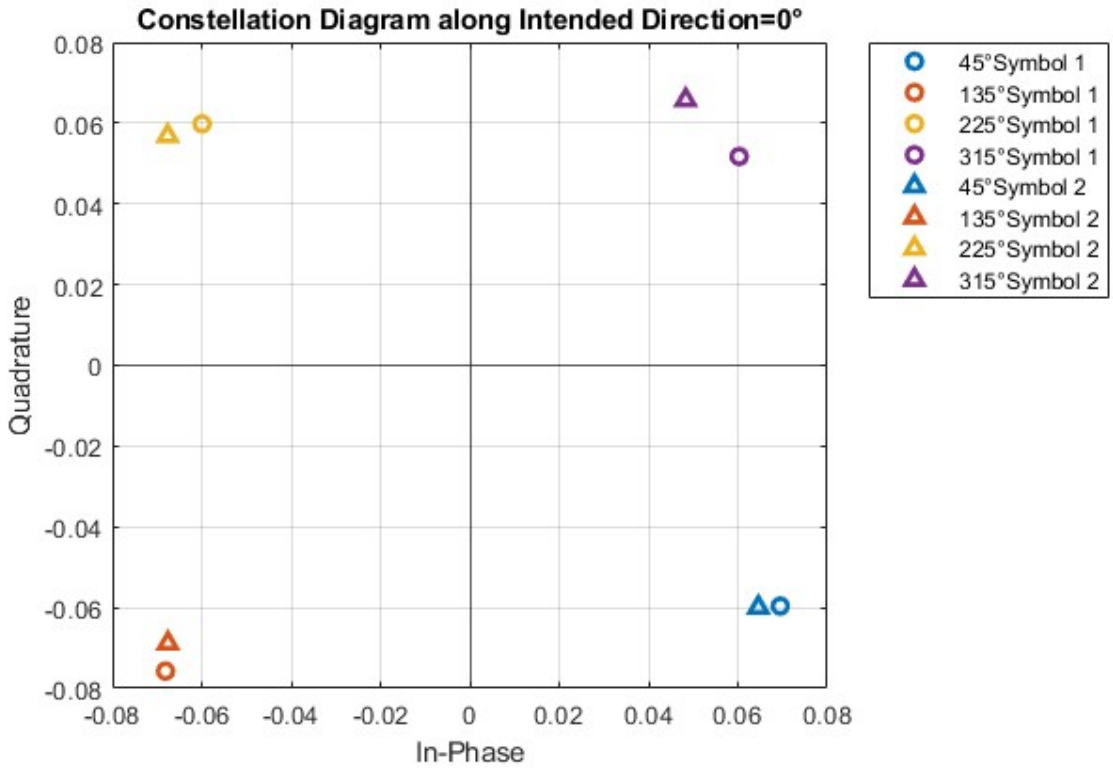

Figure 13 - Received constellation at 0° for DM weightings.

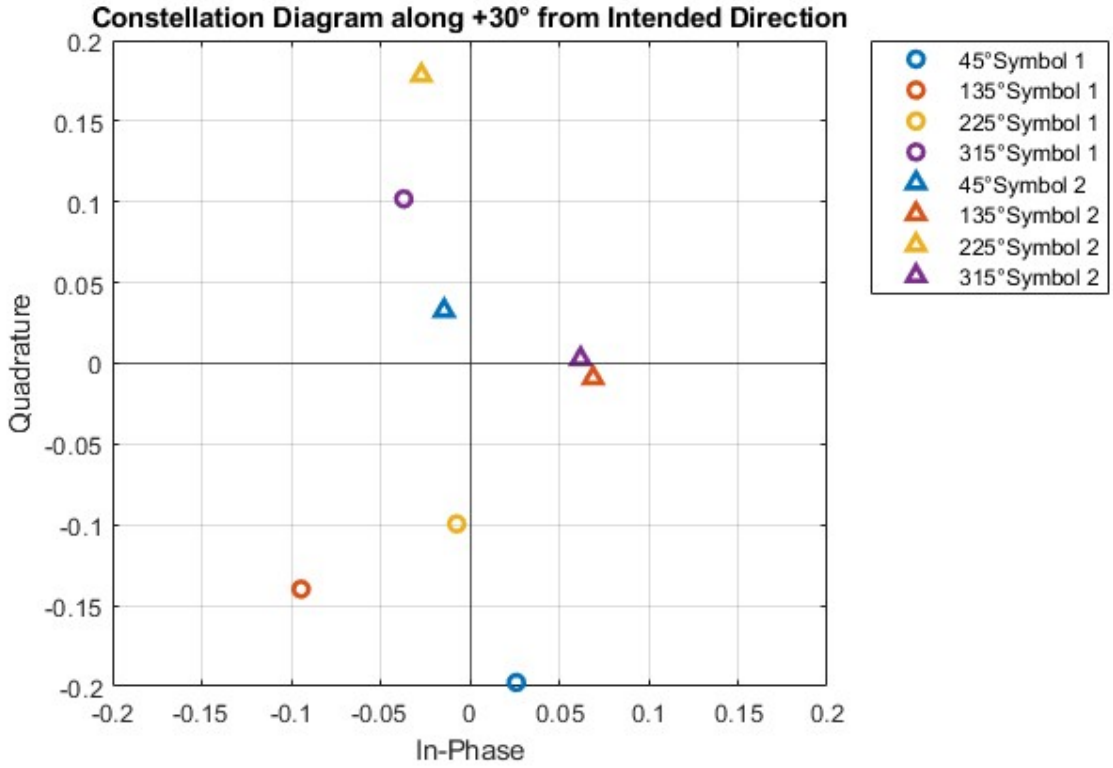

Figure 14 - Received constellations at 30° for DM weightings.

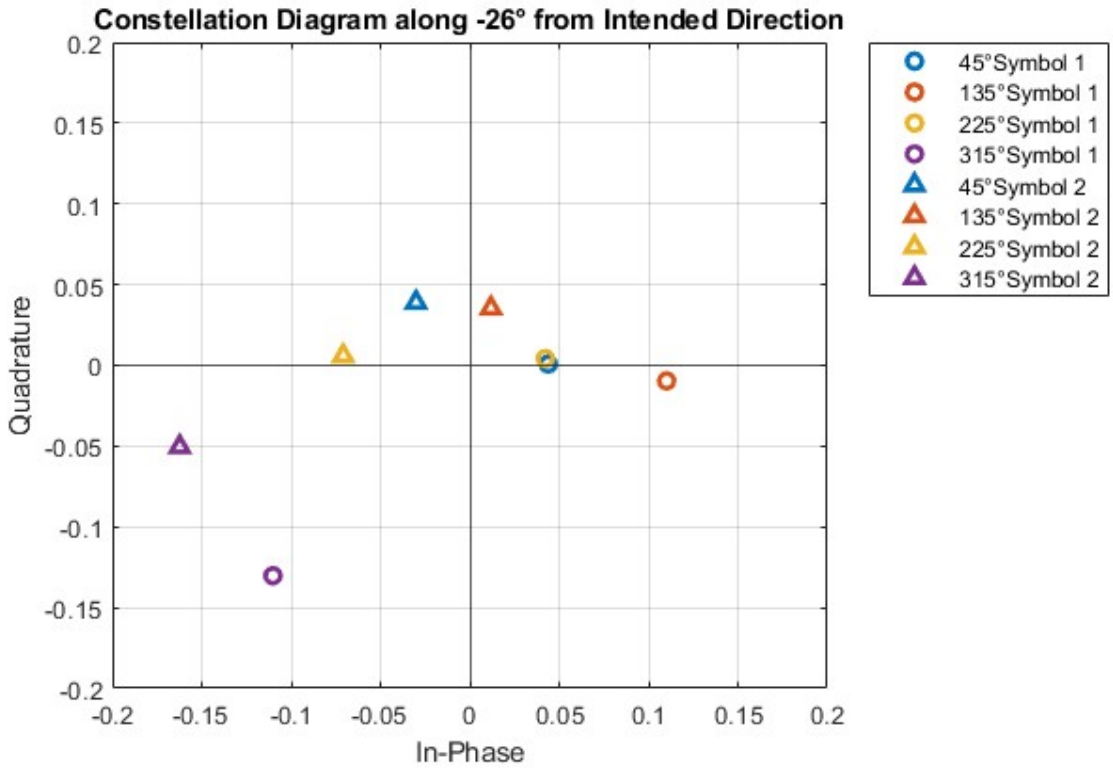

Figure 15 - Received constellation at -26° for DM weightings.

To gain appreciation for how this arrangement offers additional security to that of a traditionally steered phased array, the same constellation plots are shown in Figure 16, Figure 17 and Figure 18 for the case where the phase shifters were set to the same values. At 0°, the constellation is clear as it is in Figure 13, however off boresight, the constellation is still clear, with only a phase rotation and magnitude reduction, which and eavesdropper could easily counteract with sufficient knowledge of the pilot or synchronisation scheme in place.

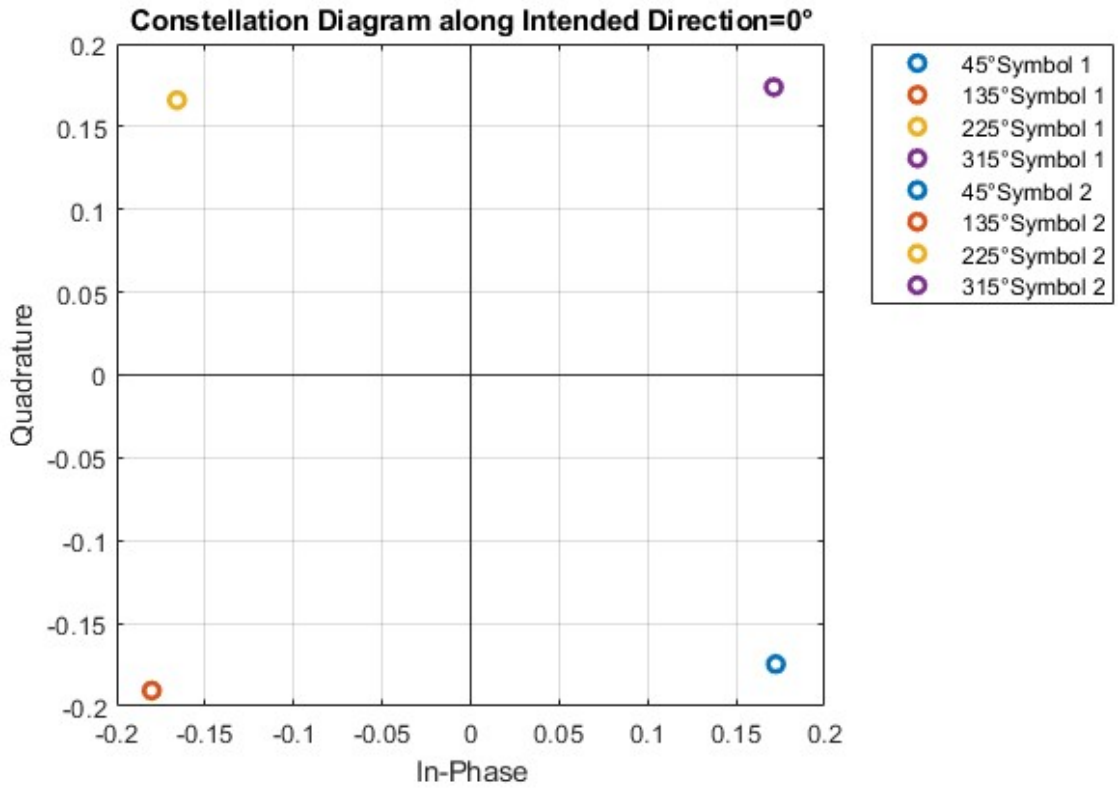

Figure 16 - Received constellation at 0° for traditional weightings.

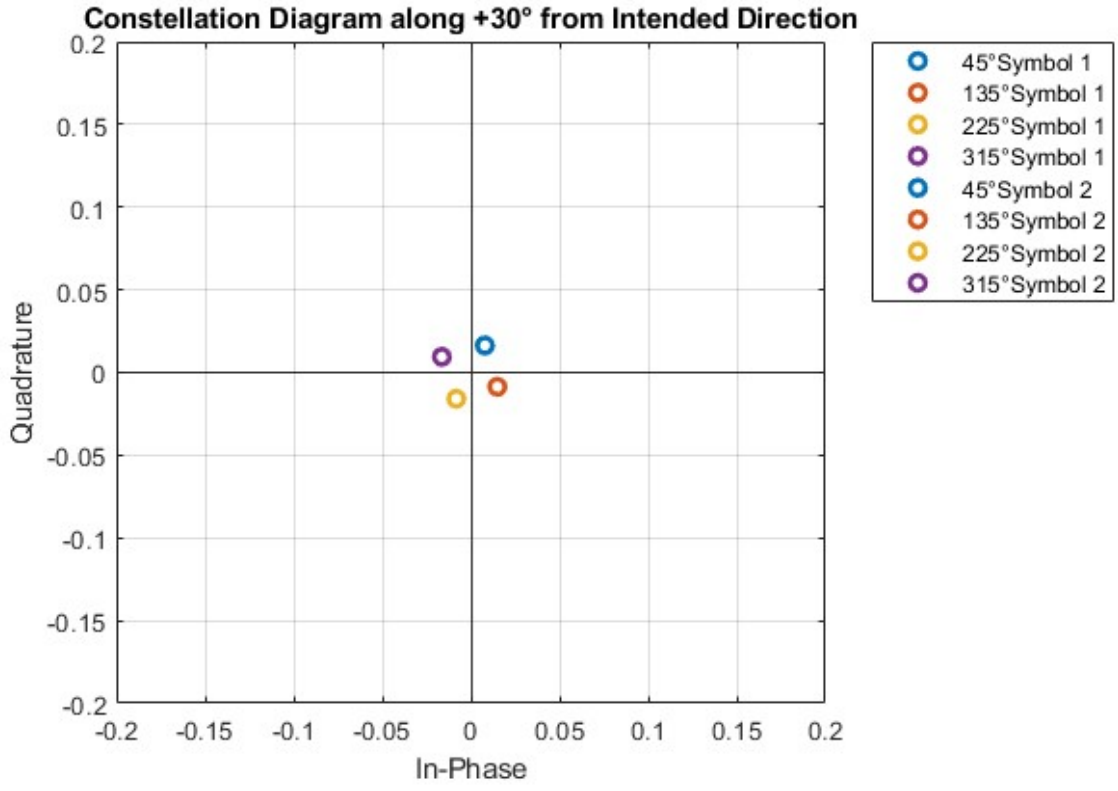

Figure 17 - Received constellation at 30° for traditional weightings.

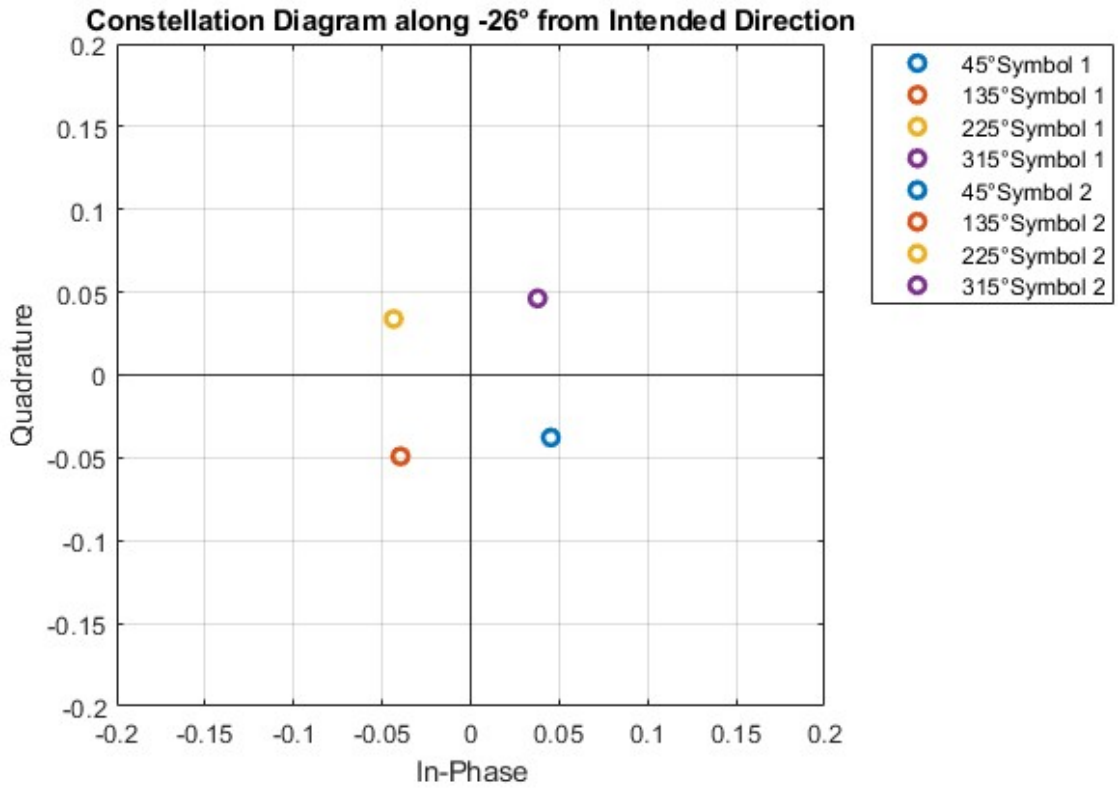

Figure 18 - Received constellation at -26° for traditional weightings.

The best indication of the security improvement provided by the DM scheme is shown in the contrast between Figure 19 and Figure 20 Since at each observation angle, the symbols were measured in the order 45°, 135°, 225°, 315°, the symbol-to-symbol transition phase is always 90° in the traditional arrangement making eavesdropping simpler due to the predictable nature of the modulation scheme, independent of observation angle. However, in Figure 20, it can be seen that the only point in azimuth space where all symbol-to-symbol transitions converge towards 90° is in the intended direction, whilst elsewhere the transition is random, meaning the channel cannot be equalised to extract the data.

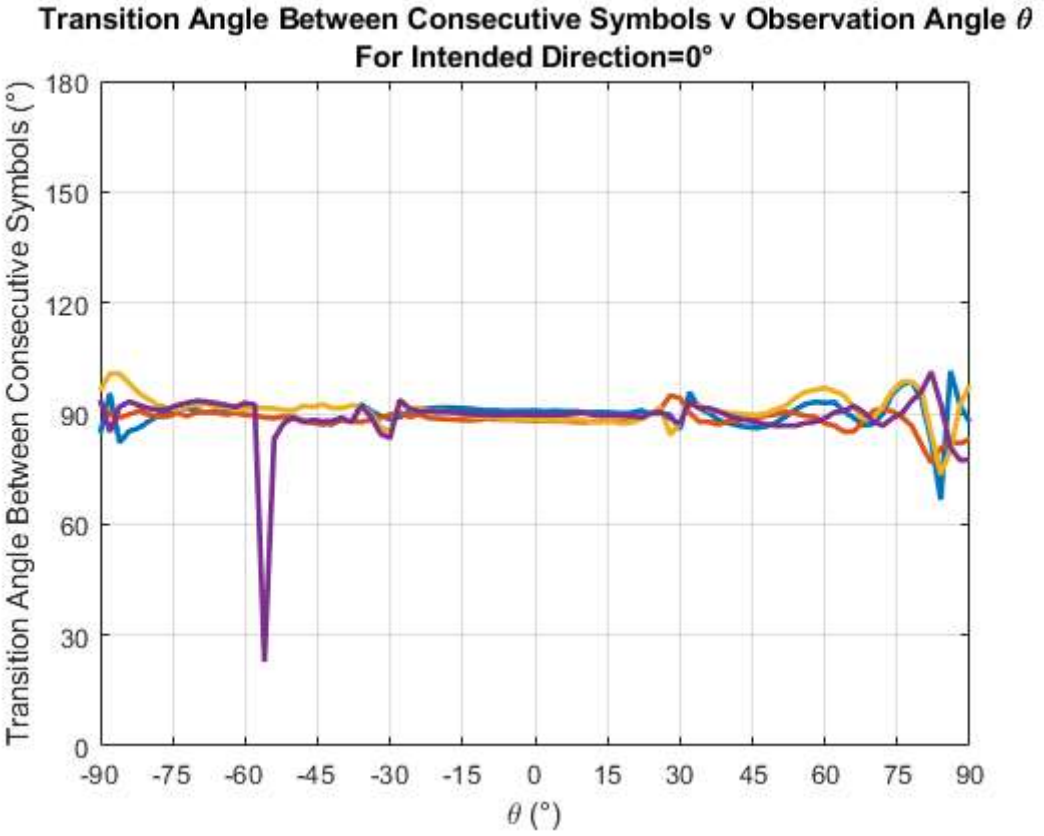

Figure 19 - Symbol-to-symbol transition angle for traditional weightings.

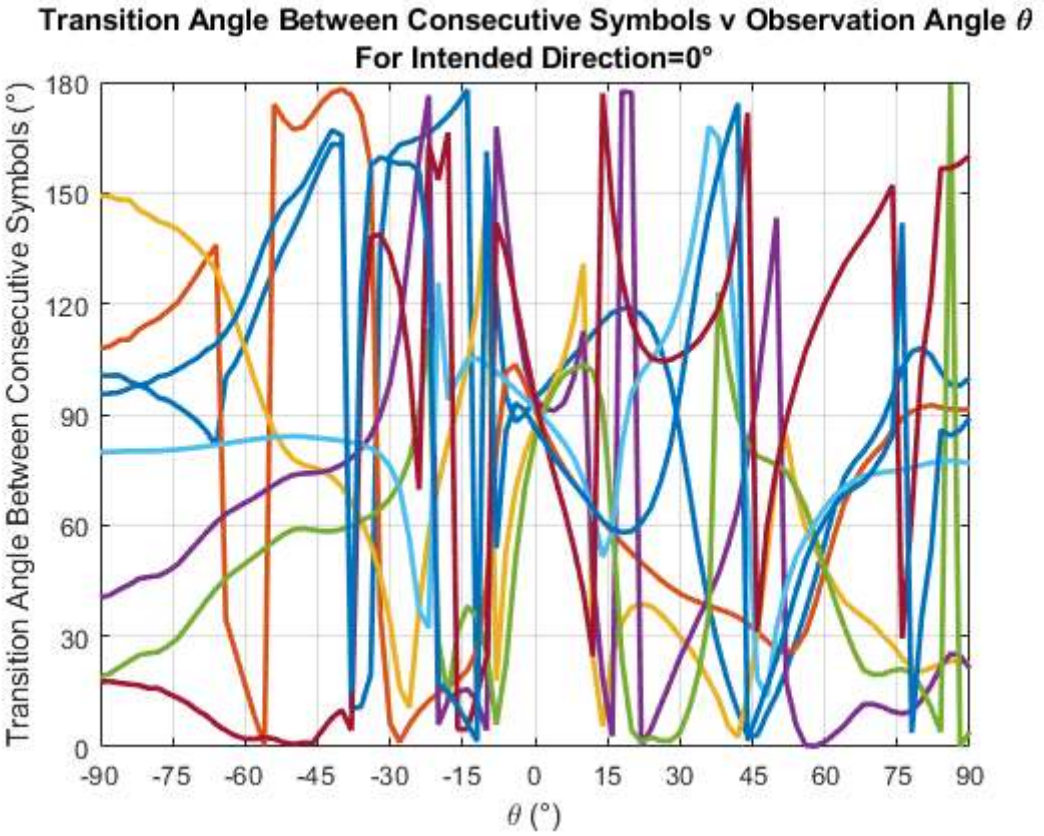

Figure 20 - Symbol-to-symbol transition angle for DM weightings.

To show that this technology is not just applicable to broadside arrays, the test was repeated with the intended direction steered to 30°, by using the same calibrated element weightings as in the original DM experiment but applying the relative phase shift between them required to steer to 30° using (7). Figure 21 shows the symbol-to-symbol transition angle comparable to Figure 20, though here the point at which the phase converges to 90° is 30° from broadside (the spread at 30° is wider since the element weightings were calibrated at 0°).

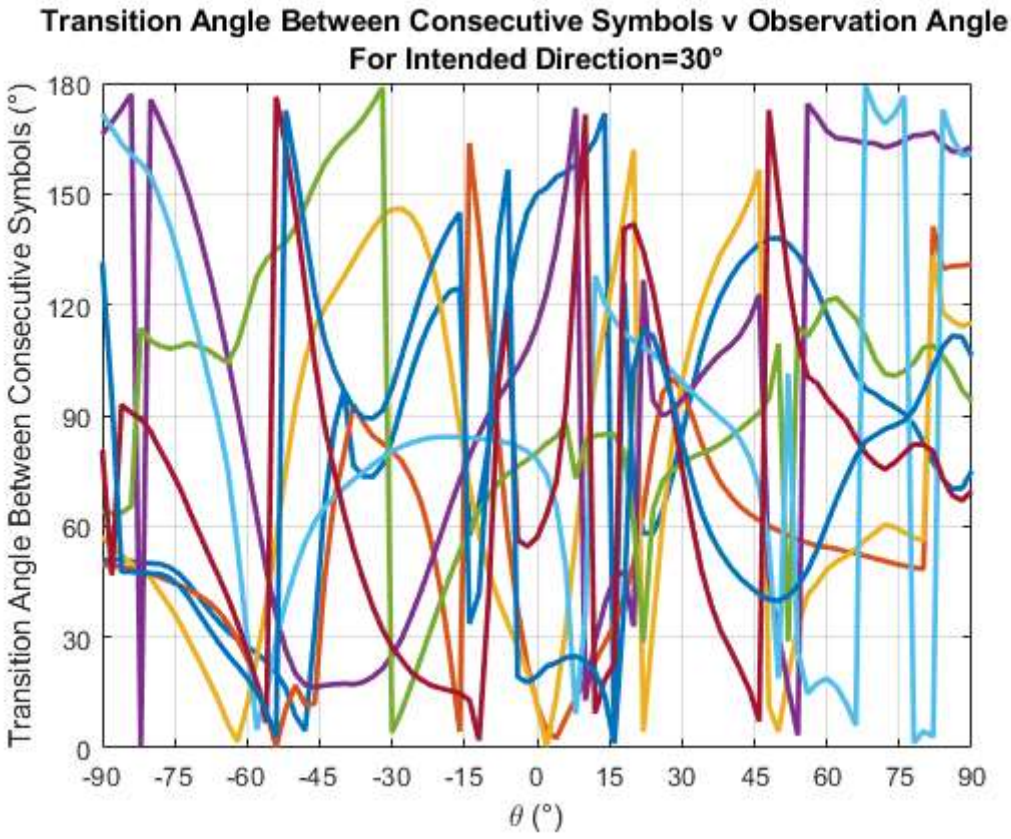

Figure 21 - Symbol-to-symbol transition angle for DM weightings steered to 30°.

Future Work

Technical Limitations

The principal trade-off in the DM scheme proposed in this paper is between information randomness in unwanted directions, and spatial power efficiency. In most combinations of element weightings that achieve sufficient randomness away from the intended receiver, the maximum energy will not be steered towards the intended receiver. Similarly, in a system which maximises energy towards the wanted direction, information in unwanted directions will be easily retrievable. Whilst this is not ideal, some applications may not require such spatial efficiency if security is a higher priority. Moreover, this paper only explores arrays with uniform amplitude for simplicity, some forms of amplitude tapering can bring an acceptable balance between in the trade-off.

Using phase shifters to modulate a carrier signal will lead to significant discontinuities in the signal and an acceptable spectral leakage in the frequency domain. Some filtering to the phase shifter values may be applied to smooth the transition from symbol-to-symbol similar to an RRC filter in the time domain, however this comes at the expense of data-rate, which is limited by the maximum switching speed of the phase shifter hardware.

Finally, the accuracy of the transmitted signal on the IQ plane, measured as EVM, is heavily reliant on the phase accuracy and stability of the phase shifters, as well as the calibration of the combination of element weightings, making this scheme impractical to modulate the carrier.

Proposed Solution

The proposed work around for the majority of these limitations is the separate the data rate from the information scrambling, which is to say remove the burden of modulation from the phase shifters.

Rather than feeding the array with a CW signal, it can be fed with a modulated signal, and the phase shifters can be used to maintain a stable far-field phase in the intended direction. Since there are many combinations of element weightings that produce the same composite phase, the weightings can be selected to always give the same phase in the intended direction, which will still have the same effect of scrambling the data in other directions. In order to combat the problem of discontinuities caused by changing of phase shifter values, a modulation scheme with a periodic energy null should be used, such as OFDM, where time domain windowing of each OFDM symbol leads to a transition period between symbols where minimal energy is transmitted. This concept is demonstrated in Figure 22, showing the magnitude of the transmitted OFDM waveform in the time domain due to windowing, along with the point in time at which the phase shifter values should be updated.

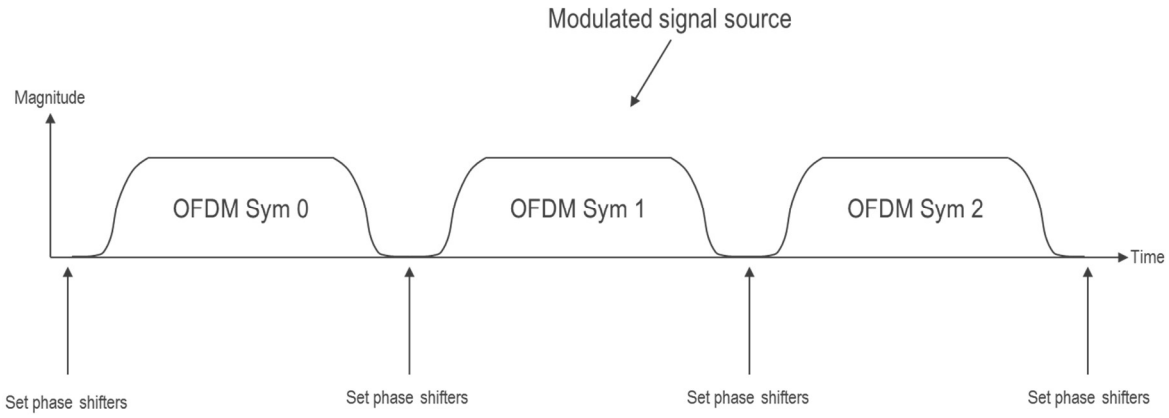

Figure 22 - Time domain OFDM symbol magnitude and phase shifter change timing.

This method separates the data rate from the 'scrambling rate', which can be updated much more slowly and removes the data rate limitation imposed by the switching speed of the phase shifters. To ensure that OFDM channel equalisation cannot be achieved by eavesdroppers to negate the security gains of the DM system, OFDM pilots should be arranged in a block format, with all subcarriers being occupied by a pilot tone at common point in time, rather than a few subcarriers carrying pilots at every time instance, since this could be used to calculate the DM phase shifters for any given symbol. This concept is shown in Figure 23.

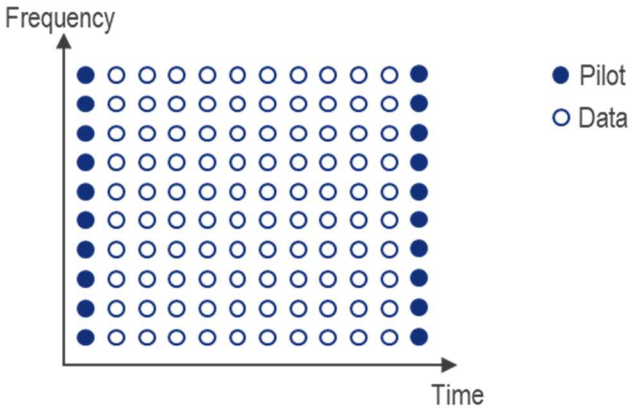

Figure 23 - OFDM block type pilot scheme.

Summary

This paper has presented the concept of DM, derived from first principles, and proven the mathematics to provide a solid platform for future theoretical development. The proof-of-concept experiment was detailed along with results and analysis, and the trade-offs and limitations of the technology have been explored with an improved solution proposed. Though this is still an area of significant research, it does present optimism for future work that will allow for spatially secure communication systems, even if the location of the transmitting array is known.